ORIGINAL ARTICLE | OPEN ACCESS

PseudoCell: A Multivalued Logical Regulatory Network to Investigate Premature Senescence Dynamics and Heterogeneity

Vinícius Pierdoná[1] 🔵 | Patrícia Lavandoski[1] | Rafael Moura Maurmann[2] | Guilherme Antônio Borges[3,4] | Jose Carlos Merino Mombach[5] | Fátima Theresinha Costa Rodrigues Guma[1] | Florencia María Barbé-Tuana[2,6]

[1]Programa de Pós-Graduação Em Ciências Biológicas: Bioquímica Do Departamento de Bioquímica, Universidade Federal Do Rio Grande Do Sul, Porto Alegre, Rio Grande do Sul, Brazil | [2]Programa de Pós-Graduação Em Biologia Celular e Molecular da Escola de Ciências da Saúde e da Vida - Pontifícia Universidade Católica Do Rio Grande Do Sul, Porto Alegre, Rio Grande do Sul, Brazil | [3]Departamento de Engenharia Electrotécnica e de Computadores, Universidade de Coimbra, Coimbra, Portugal | [4]Departamento de Ensino, Pesquisa e Extensão - Instituto Federal Sul-Rio-Grandense, Campus Charqueadas, Porto Alegre, Rio Grande do Sul, Brazil | [5]Departamento de Física, Universidade Federal de Santa Maria, Santa Maria, Rio Grande do Sul, Brazil | [6]Programa de Pós-Graduação Em Pediatria e Saúde de Criança da Escola de Medicina, Pontifícia Universidade Católica Do Rio Grande Do Sul, Porto Alegre, Rio Grande do Sul, Brazil

Correspondence: Florencia María Barbé-Tuana (florencia.tuana@pucrs.br)

ABSTRACT

Purpose: Premature cellular senescence is a pivotal process in aging and age-related diseases, triggered by various stressors. However, this is not a homogeneous phenotype, but a heterogeneous cellular state composed of multiple senescence programs with different compositions. Therefore, understanding the complex dynamics of senescence programs requires a systemic approach. We introduce PseudoCell, a multivalued logical regulatory network designed to explore the molecular intricacies of premature senescence.

Methods: PseudoCell integrates key senescence signaling pathways and molecular mechanisms, offering a versatile platform for investigating diverse premature senescence programs initiated by different stimuli.

Results: Validation through simulation of classical senescence programs, including oxidative stress-induced senescence and oncogene-induced senescence, demonstrates its ability to replicate molecular signatures consistent with empirical data. Additionally, we explore the role of CCL11, a novel senescence-associated molecule, through simulations that reveal potential pathways and mechanisms underlying CCL11-mediated senescence induction.

Conclusions: In conclusion, PseudoCell provides a systematic approach to dissecting premature senescence programs and uncovering novel regulatory mechanisms.

1 | Introduction

Cellular senescence is a cell state that entails the permanent cell cycle arrest associated with chronological aging and multiple aging-related diseases. Premature senescence can be initiated by various exogenous or endogenous stress-induced insults. This phenotype is associated with a shift in the cellular morphological and metabolic landscape, including accumulation of macromolecule damage and establishment of the senescence-associated secretory phenotype (SASP) [1–3]. Mechanistically, this phenotype triggers multiple, heterogeneous, and context-dependent senescence programs to achieve its cellular outcome. These molecular programs can be composed of different signaling pathways and partially depend on specific senescence-inducing stimuli [2, 4].

Considering this perspective, the systemic paradigm aimed to provide a theoretical framework that can account for the inherent stochasticity of complex biological phenotypes [5, 6]. Within this perspective, the in silico study of biological networks presents itself as a powerful tool to structure and analyze the spatial and dynamic organization of these biological systems [7–11]. Among the existing methodologies and formalisms in this field, the logical modeling of the biological networks stands out given its flexibility and high predictive power [12–19].

In logical modeling, each biological entity is represented as a node or a vertex in a graph and is associated with a discrete variable representing its activation state. The relationships between these elements are represented as links or edges in the graph and are described as logical functions. This structure allows computing the state transition of a given node in the face of changes in neighboring regulatory nodes [17, 18, 20, 21]. Therefore, logical modeling of biological systems is an alternative for understanding the molecular dynamics established in complex phenotypes, such as premature senescence, from a systemic perspective.

In this sense, the proposition of a logical model that encompasses the main senescent mechanisms to determine the dynamics described by premature senescence programs holds significant promise for unraveling the biological complexity inherent to these processes. In this work, we present PseudoCell, a multivalued logical regulatory network built to assist the investigation of the different dynamics in premature senescence and unfold its intrinsic heterogeneity.

2 | Model Scope and Definition

The scope of a model guides the selection of its elements, encompassing the array of regulatory pathways and biological entities essential for the modeled biological phenomena [21]. Therefore, in investigating the dynamics underlying the establishment of premature senescence in humans, it is imperative to identify the relevant pathways involved and elucidate their interconnections.

Macromolecular damage, especially to genomic material, is an important marker in many senescence programs. Cellular insults such as oxidative stress act as agents that potentially compromise genomic integrity [1, 3]. The accumulation of DNA damage leads to the mobilization of a complex repair machinery, collectively called DNA Damage Repair (DDR). In general, the propagation of DNA damage by genotoxic agents converges on the phosphorylation of the protein tumor protein P53 (TP53) mediated by ATM serine/threonine kinase (ATM) or ATR serine/threonine kinase (ATR) [22–24]. Activation of TP53 leads to activation of cyclin-dependent kinase (CDK) inhibitors, such as CDK Inhibitor 1A (p21^{CIP1}) [25]. The activation of proteins from the CDK inhibitors family mostly leads to cell cycle arrest through hypophosphorylation of retinoblastoma protein (pRb) [26].

Among the effector mechanisms of macromolecular damage, it is important to consider the role of oxidative stress. Normal reactive oxygen species (ROS) levels are important for maintaining homeostatic cellular processes. However, this system must be maintained by a delicate balance, supported by enzymatic and nonenzymatic antioxidant defense mechanisms [27]. The dysregulation of these mechanisms leads to the promotion of oxidative stress, with damage to macromolecules and the expression of pro-inflammatory factors. Indeed, evidence indicates that ROS is an important factor in multiple senescence programs [28].

Furthermore, inflammation promotes the senescent phenotype and macromolecular damage alone or in conjunction with ROS. For example, oxidative stress is responsible for increasing the production of damage-associated molecular patterns (DAMP), which act by increasing the expression of cytokines mediated by receptors such as Advanced Glycosylation End-Product Specific Receptor (RAGE) [29, 30]. Concomitantly, evidence indicates that the expression of inflammatory mediators [31] leads to the consolidation of an oxidative phenotype. In this sense, inflammation and oxidative stress form an interdependent phenotype whose apex is the accumulation of DNA damage [32, 33].

Furthermore, an important marker for many senescence programs is the consolidation of the SASP. SASP is characterized by the highly heterogeneous secretion of multiple soluble factors, including proinflammatory cytokines and chemokines, growth factors, and metalloproteinases [34]. Evidence indicates that an important factor in the construction of this phenotype is DDR, which signals through NF-kB [35] to assemble most of the secretory phenotype. Therefore, this causal relationship between DNA Damage and SASP through NF-kB draws an intrinsic parallel between this phenotype and the proinflammatory and pro-oxidative pathways in the formation of senescence. However, using SASP as a senescence marker is limited by its high heterogeneity [4, 34]. Therefore, understanding how these secretory patterns relate to different senescence programs requires a systemic analysis.

In this sense, PseudoCell was modeled to comprehend pathways associated with DDR, oxidative stress, and inflammation. Currently, the PseudoCell network consists of 594 nodes connected by more than 2.000 directional edges (Figure S1). A comprehensive list of the network components, their descriptions, and the references are available at the PseudoCell website.

3 | Logical Formalism

In logical modeling, regulatory networks are depicted as a graph, $G = (V, E)$, where V defines the vertices or nodes, and E represents the links or edges. Each node in this model represents a biological entity involved in the phenomenon under study, such as genes or proteins. Conversely, the links or edges abstractly represent the activation or inhibition mechanisms between two network elements [20, 36]. Also, network nodes are associated with discrete variables x_i that qualitatively represent the activation level of the corresponding element [20]. Generally, a node's activation state represents the threshold beyond which the element initiates a specific biological function. In multivalued networks, such as PseudoCell, the activation state of a given node is represented by a numerical value, assuming values in the range $x_i = [0, Max_n]$, where Max_n is the maximum state value described for that component.

Finally, to each node is assigned a logical function to determine its activation state x_i at a given time. The state of the logical network, at a given moment in time t, will be defined by a vector of activation states $\overrightarrow{X}(t) = (x_1(t), x_2(t), x_3(t), \dots, x_n(t))$, where n is the number of nodes in the network [37]. However, the transition between states in a logical network depends not only on the set of logical functions that constitute it but also on the node update scheme applied. PseudoCell applies a random order asynchronous update scheme where, in each update round, the nodes are randomly organized into a list and then updated. The resulting dynamics can thus be evaluated throughout the system's evolution, after a certain arbitrary period.
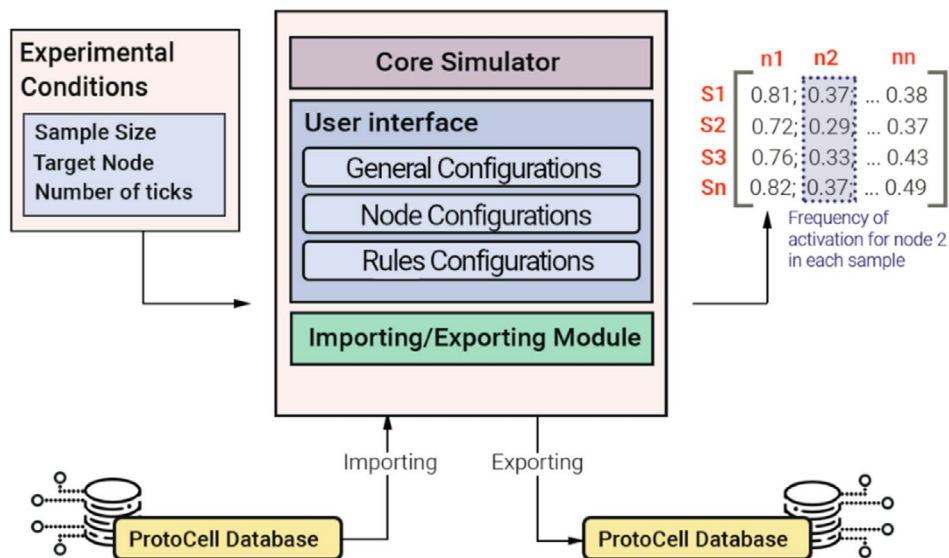
4 | PseudoCell Interface

PseudoCell also implements its own open-source analysis and simulation interface, written in Java, that allows users to evaluate the dynamics of the regulatory network in response to perturbations at specific nodes over time (Figure 1). This interface allows users to analyze PseudoCell network node behavior in different molecular contexts, such as overexpression of a protein or knockout of a gene. In this sense, through its interface, PseudoCell allows the user to define an external stimulus frequency to any element of the network (input). The stimulus frequency is measured in activation percentage (0%–100%) and determines how many times that element (input) will be activated throughout the simulation.

In the PseudoCell interface, the execution time, or the number of rounds of updates that the simulation will undergo before stopping (called ticks), is defined by the user, and the simulation results are represented in the form of node activity frequency (NAF). The NAF represents the sum of the activation states that the node obtained throughout the simulation divided by the simulation time. This means that a dichotomous node (activation states ranging from 0 to 1) with an NAF of 0.87 was activated 87% of the time during the simulation. Due to the inherent stochasticity of the update scheme implemented in PseudoCell, NAF results may vary in two different simulations. This variation is important, as it brings the results of the logical model closer to its biological counterpart. To assess this variability, the user can define the number of repetitions for the simulation. Each repetition is called a sample, and the set of samples is called an experiment. This measure, therefore, allows the semiquantitative assessment of the dynamics established by the network. It is important to note that literature corroborates these simulation strategies, as important tools in the field, such as CellCollective, use them [8].

Upon completion of the experiment, the tool generates a matrix where the rows correspond to the result array of each sample (S1, S2...Sn). This matrix is then exported as a Comma Separated Values (CSV) file for user analysis. In addition, the PseudoCell interface also generates a CSV file where it reports the state of all network nodes after each update cycle. From this file, the

FIGURE 1 | PseudoCell interface architecture. The interface is organized into three modules: User Interface, Core Simulator, and Importing/Exporting Module. The User Interface module is responsible for handling the user's experimental conditions. The Core Simulator module is responsible for carrying out the network update iterations based on the logic rules described. The Import/Export Module handles the functions for sharing the networks created by the community. The interface returns a matrix of activation frequency values as output, where the lines represent the samples (S1, S2....Sn) and the columns (n1, n2...nn) the network nodes.

FIGURE 2 | Legend on next page.

FIGURE 2 | In silico stimulation of OSIS, OIS Ras and OIS AKT1-dependent leads to activation of molecular elements similar to those expected in biological models. (A) Heatmap demonstrating the systemic response of the network to 50% frequency stimulus of the CYBB node. In the graph, the lines represent the network nodes, while the columns represent the samples from both experimental groups. (B) Volcano plot representing differential activation nodes in OSIS group compared to the control. Red circles indicate nodes with a p value <0.010 and a fold change greater than 0.050. Yellow circles represent nodes with only a p value <0.010 and were not considered differentially activated. Gray circles represent no differentially activated nodes. (C) OSIS leads to the expression of DNA damage and cell cycle arrest markers. (D) OSIS leads to increase in p16 activation and decrease in CDK4. (E) OSIS leads to SASP factors expression. (F) Heatmap demonstrating the systemic response of the network to constitutive Ras activation. (G) Volcano plot representing differential activation nodes in Ras stimulated group compared with the control. (H) Heatmap demonstrating the systemic response of the network to constitutive AKT1 activation. (I) Volcano plot representing differential activation nodes in AKT1 stimulated group compared with the control. Data are presented as median and IQR. Significant differences considered p value <0.001 (***) and p value <0.0001 (****). Normality data distribution was assessed using the Shapiro–Wilk normality test. Mann–Whitney U-test was used for nonparametric samples. NAF, node activation frequency.
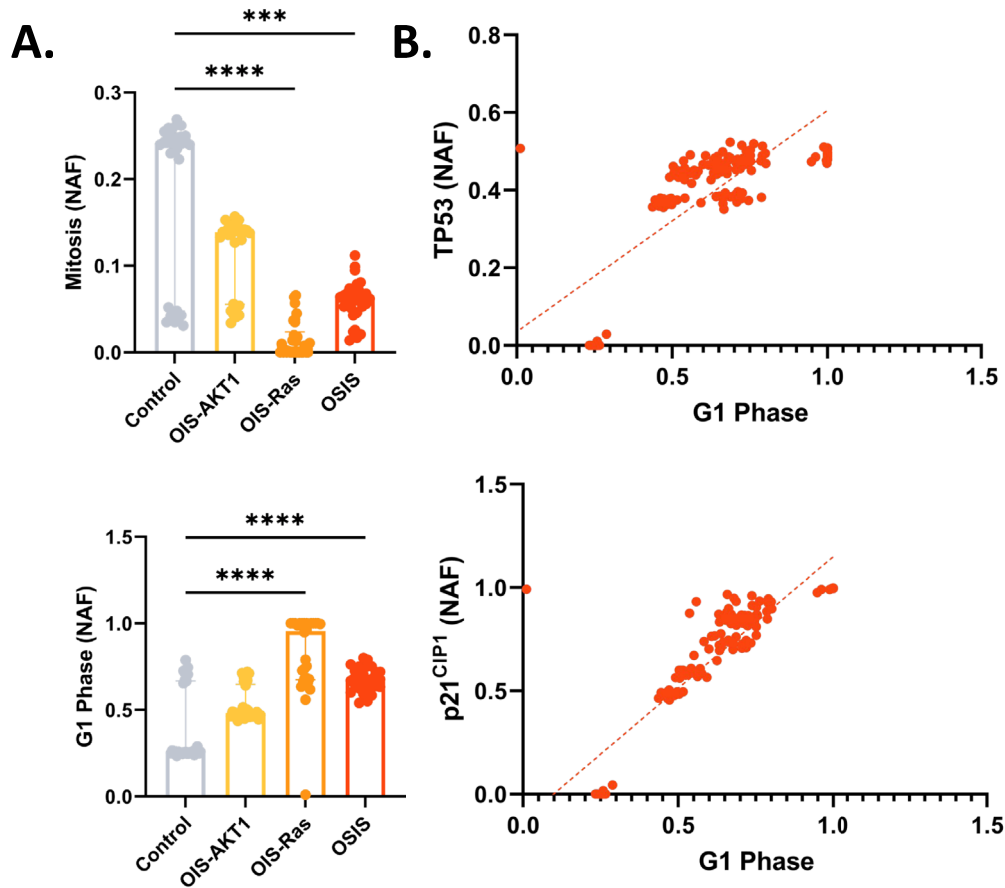
FIGURE 3 | In silico cell cycle arrest simulation in different premature senescent models. (A) Increased activation of the G1 Phase node in most senescence-inducing stimuli and reduced mitosis. (B) Positive correlation between G1 cell cycle arrest and TP53 or p21 activity. Data distribution normality assessed by the Shapiro–Wilk test. Intergroup differences assessed by the Kruskal–Wallis test followed by comparison of each group's mean rank with the rank of the control group. The data presented are expressed as the median and Interquartile Range. Significant differences considered when p value <0.001 (***) or p value <0.0001 (****). NAF, node activation frequency.

user can determine the update cycle at which the nodes of the network entered stability or reached a steady state.

5 | Validation of PseudoCell Through Simulation of Classical Senescence Programs

To assess the accuracy of PseudoCell, we conducted simulations replicating classical senescence programs. Specifically, we emulated oxidative stress-induced senescence (OSIS) by perturbing the node related to NADPH Oxidase 2 (CYBB) at a frequency of 50% and oncogene-induced senescence (OIS) by constitutive expression of AKT1 and Ras nodes. All simulations were maintained for 1.000 ticks and were repeated 30 times ($n = 30$). The network's NAF were expressed as a heatmap where the rows represent the nodes and the columns represent the experimental groups. Subsequently, we compared the nodes modulated by each of the stimuli with empirical data available in literature.
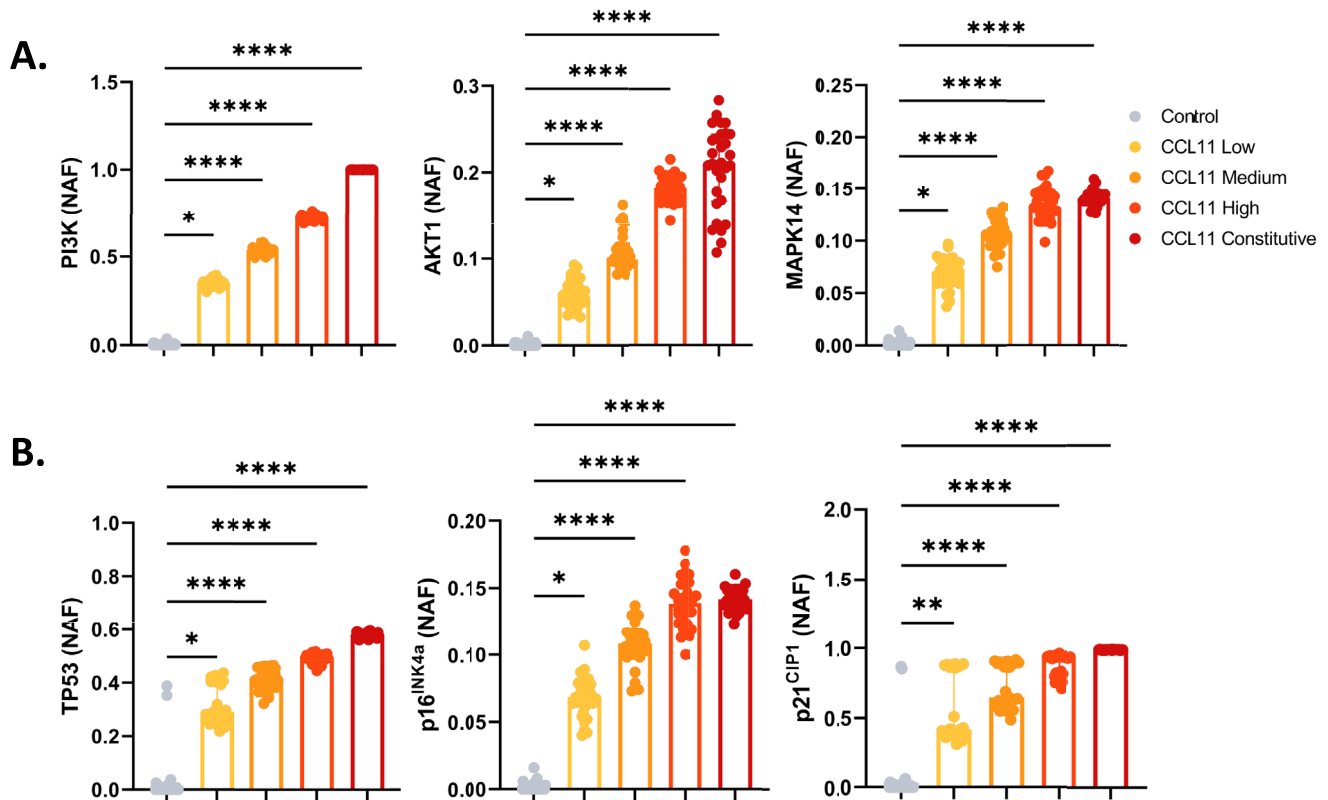
FIGURE 4 | CCL11 induces activation of nodes associated with PI3K/AKT, MAPK14, and cell cycle arrest pathways in PseudoCell's network. (A) The PI3K, AKT1, and MAPK14 nodes had their activity modulated in a frequency-dependent manner when disturbed by CCL11. (B) Activation of TP53, p16, and p21 node after CCL11 stimulation. Data distribution normality assessed by Shapiro–Wilk test. Intergroup differences assessed by Kruskal–Wallis test followed by comparison of each group's mean rank with the rank of the control group. Significant differences considered when p value < 0.050 (*), p value < 0.010 (**), and p value < 0.0001 (****). NAF, node activation frequency.

To determine which nodes had their activities modulated by the provided perturbations, we verified the node differential activation using R language and the clusterProfiler [38, 39] and limma packages [40].

5.1 | Validation of Oxidative Stress-Induced Senescence Molecular Signature

In the OSIS model, the stimulation of the CYBB node resulted in increased activity of proteins associated with DDR and cell cycle arrest, such as H2AX, ATM, MDC1, TP53BP1, TP53, and p21[CIP1] (Figure 2A–C and Table S1). Interestingly, these findings are in line with the molecular markers commonly found in cellular senescence induced under pro-oxidative conditions. While low to moderate levels of ROS serve as essential signaling molecules involved in cellular homeostasis and adaptive responses, excessive ROS accumulation can induce oxidative damage to biomolecules, ultimately leading to cellular dysfunction and senescence. Accumulation of oxidative stress-derived DNA damage triggers DDR signaling, phosphorylating H2A Histone Family Member X (γH2AX), while also activating ATM, TP53BP1, and MDC1 [28, 41, 42]. As in our model, DDR signaling converges on the phosphorylation of TP53 leading to p21[CIP1] expression and cell cycle arrest [43, 44]. Moreover, evidence indicates that ROS-mediated activation of p16[INK4a] and inhibition of CDK4 and 6 are

also important in the consolidation of the senescent phenotype under oxidative stress [45, 46]. These elements were also found to respond to in silico CYBB stimulation in our model (Figure 2D). Lastly, we observed the expression of SASP-associated markers, including NF-kB [47] (Figure 2E). These in silico results support the idea that our model is capable of producing a molecular activation profile mirroring the response seen in living organisms after exposure to an oxidative stressor.

5.2 | Validation of Oncogene-Induced Senescence Molecular Signature

Furthermore, we also assessed the network's response to the overexpression of two senescence-associated oncogenes, Ras and AKT1. OIS represents a critical tumor suppressive mechanism that acts as a barrier to tumorigenesis. Similar to stress-induced senescence, upon Ras superexpression (OIS-Ras), the cell undergoes DNA damage and oxidative stress pathway activation, leading to upregulation of TP53, p16[INK4a], and SASP factors [48]. The p16[INK4a] tumor suppressor pathway acts as a critical regulator of OIS by inhibiting the activity of CDK4 and CDK6, thereby preventing the phosphorylation of Rb and subsequent cell cycle progression. In our model, we also observed the modulation of these markers mediated by the constitutive expression of Ras (Figure 2F,G and Table S2).
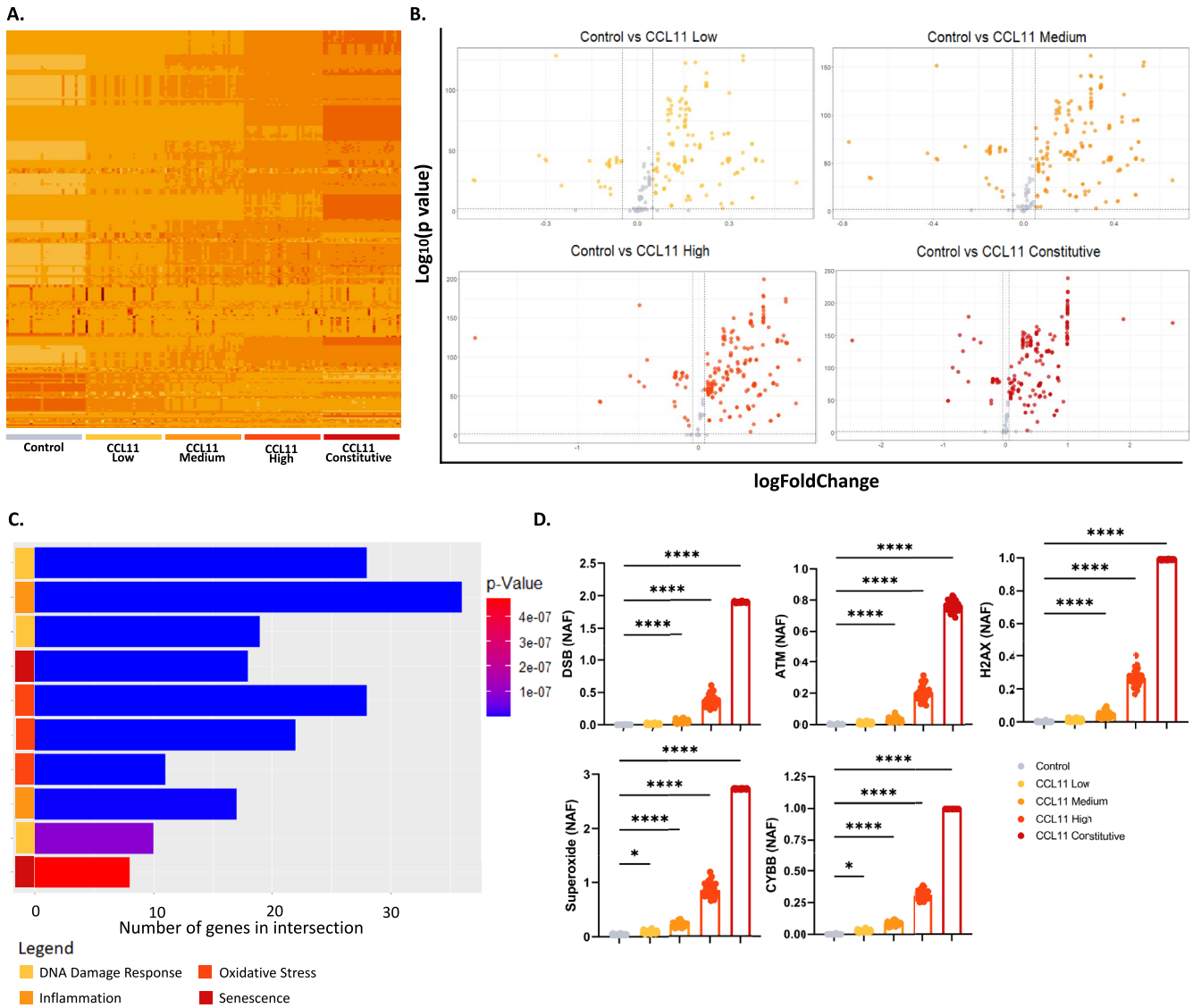
FIGURE 5 | In silico evaluation of increasing frequency of CCL11 node activation. (A) Heatmap representing alteration in activation frequency patterns for Control, CCL11 Low, CCL11 Medium, CCL11 High, and CCL11 Constitutive groups. (B) Volcano plot showing the differentially activated nodes in Controls in contrast to CCL11 Low, Medium, and Constitutive (p value < 0.010 and |FC| > 0.050). Negative FC values were considered downregulated, while positive values were considered upregulated. (C) Top enriched pathways in CCL11 High. (D) CCL11 activation frequencies induce an increase in DSB, ATM, H2AX, Superoxide, and CYBB nodes activation (p value < 0.0001). Data distribution normality assessed by Shapiro–Wilk test. Intergroup differences assessed by Kruskal–Wallis test followed by comparison of each group's mean rank with the rank of the control group. Significant differences considered when p value < 0.050 (*), p value < 0.010 (**), and p value < 0.0001 (****). NAF, node activation frequency.

Contrastingly, in the AKT-induced senescence (OIS-AKT1) model, the overexpression of the oncogene AKT1 leads to the consolidation of senescence through a distinct phenotypic pattern. Significantly, AKT1 overexpression contrasts with Ras-dependent OIS and OSIS by not involving the activation of pathways associated with DNA damage. Evidence indicates that AKT1 overexpression induces senescence through TP53 mTORC1-dependent activation and reduction of MDM2 activity in the absence of DNA damage [49, 50]. Moreover, in contrast to other models, cell cycle arrest in OIS-AKT1 mediated appears to be dependent on p21$^{\text{CIP1}}$, with no involvement of p16$^{\text{INK4a}}$. Interestingly, our model was able to replicate these differences found among different senescence programs, indicating activation of the PI3K/AKT/mTORC1 pathway and markers such as TP53 and p21 without activation of DNA damage markers like H2AX and p16 (Figure 2H,I and Table S3). Also, findings

suggest that OIS AKT1-induced leads to NF1-dependent suppression of Ras signaling [51].

5.3 | Senescence Inducing Stimuli Leads to G1 Cell Cycle Arrest In Silico

Additionally, most senescence-inducing stimuli tested in our model led to an increase in G1 node activity, associated with reduced mitosis (Figure 3A). This is an important finding as many senescence models indicate G1 cell cycle arrest. For example, human fibroblasts subjected to gamma radiation-induced senescence exhibited G1 cell cycle arrest dependent on DNA damage and prolonged activation of TP53 and p21$^{\text{CIP1}}$ [52]. Furthermore, the cell cycle arrest in G1 positively correlates with the activity of the p21$^{\text{CIP1}}$ and TP53 nodes in our

model, replicating the expected behavior in a biological system (Figure 3B).

Collectively, these findings demonstrate that PseudoCell is capable of satisfactorily emulating different programs of OSIS and OIS, thereby providing insights into the molecular mechanisms underlying each senescence program.

6 | Validation: Exploring the Role of CCL11 in Cellular Senescence

Recent literature suggests that CCL11 acts as a premature aging factor central in aging-related pathological conditions, such as severe or treatment-refractory asthma. In these individuals, levels of CCL11 circulating in peripheral blood are negatively correlated with telomere length [53]. Furthermore, evidence corroborates the association of CCL11 with aging and senescence by demonstrating the age-dependent increase of this molecule in human peripheral blood [54]. Despite this, little is known about the molecular and intracellular events that explain the association of this chemokine with cellular aging.

To validate the PseudoCell regulatory network's capacity to assist in the study of novel molecules in premature senescence induction, we sought to evaluate molecular aspects associated with increasing concentrations of CCL11. For this purpose, PseudoCell was stimulated with perturbations of the CCL11 node at increasing frequencies: 100% (constitutive expression), 50% (high expression), 25% (medium expression), 12.5% (low expression), and 0% (control). The network was then updated for 1.000 ticks, and the simulations were repeated 30 times ($n = 30$) for each experimental group.

Initially, we sought to verify if the in silico stimulation with CCL11 was able to replicate empirical results found in the literature. For that, we assessed the activation frequency of nodes associated with the PI3K/AKT and MAPK14 pathways. In this experiment, we verified a frequency-dependent increase in PI3K, AKT1, and MAPK14 nodes (Figure 4A). These results align with the literature, where an increase in the expression or phosphorylation of these proteins was observed after stimulation with CCL11, evidencing the accuracy of our model in emulating the CCL11 biological function in silico [55–58]. Furthermore, corroborating its role as a potential inducer of senescence, we also verified the expression of classical markers of multiple senescence programs such as TP53, p21^{CIP1}, and p16^{INK4a} (Figure 4B). Being able to replicate the aging phenotype promoted by CCL11, we sought to understand which mechanisms could explain this phenomenon.

Therefore, we assess the molecular signature promoted by stimulation at increasing frequencies with CCL11 and investigate the possible mechanisms responsible for CCL11-mediated senescence induction (Figure 5A and Table S4). To assess the consequences of CCL11 stimulation, we investigate the differentially activated nodes in the experimental groups compared to the control (Figure 5B). Sequentially, we evaluated the signaling pathways enriched in this list of genes and proteins. Our results show an important prevalence of pathways associated with DNA damage and repair (Figure 5C and Table S5). This finding is expressed by an increased frequency of activation of nodes such as Double Strand Break (DSB), ATM, and H2AX. Furthermore, there was an increase in the node activation associated with the ROS production pathway and the gene that codify for NADPH oxidase 2 (CYBB) (Figure 5D). Furthermore, these results were validated in peripheral blood mononuclear cells (PBMC) in vitro (Figure S2).
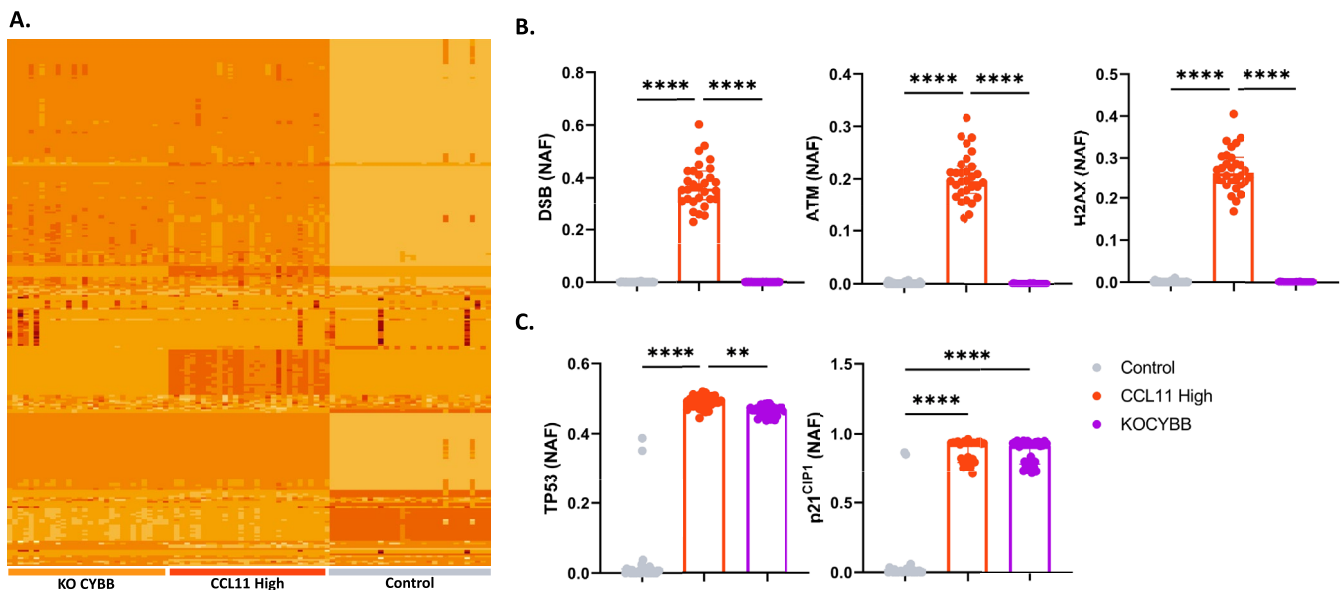
FIGURE 6 | Effects of CYBB node suppression on DNA damage response and senescence markers. (A) Heatmap representing alteration in activation frequency patterns for Control, CCL11 High, and CYBB Knockout (KO CYBB) groups. (B) CYBB knockout suppresses activation of nodes associated with DNA damage, DSB, ATM, and H2AX. (C) CYBB knockout reduces TP53 activation, but not p21. Data are presented as median and IQR. Data distribution normality was assessed by Shapiro–Wilk test. Intergroup differences were assessed by Kruskal–Wallis test. Significant differences were considered p value < 0.010 (***), and p value < 0.0001 (****). NAF, node activation frequency.

To verify the causal relationship between ROS production in CCL11 pathway activation and the promotion of DNA damage, the system was challenged with increasing frequencies of CCL11 node activation associated with CYBB node knockout. The results were expressed in a heatmap (Figure 6A). In this analysis, CYBB knockout inhibited the activation of nodes associated with the DNA damage response (Figure 6B). Furthermore, inhibition of oxidative stress CCL11-induced production also led to reduced activation of TP53, but not p21^{CIP1} (Figure 6C). This indicates that ROS production has a partial role in the induction of senescence mediated by CCL11. These findings indicate that CCL11 induces a senescent phenotype with involvement of ROS formation and DNA damage, similar to that induced by cellular stress.

7 | Conclusion

In this study, we introduced PseudoCell, a multivalued logical regulatory network designed to unravel the dynamics underlying cellular senescence. By comprehensively integrating key signaling pathways associated with senescence, PseudoCell offers a versatile platform for investigating the diverse senescence programs initiated by various cellular stimuli. Our analysis demonstrated that PseudoCell accurately recapitulates classical senescence programs by replicating molecular signatures consistent with empirical observations. Furthermore, we validated the utility of PseudoCell in exploring the role of novel molecules in cellular senescence.

It is important to note that PseudoCell does not claim to encompass all mechanisms associated with senescence in its current version. For instance, telomeric dynamics are not explicitly included in our model. However, future iterations of PseudoCell can expand its scope to incorporate additional components and refine existing interactions.

In conclusion, PseudoCell emerges as a resource for investigating the complex dynamics of cellular senescence, offering a systematic approach to dissecting premature senescence programs and uncovering novel regulatory mechanisms.

Ethics Statement

Methods were conducted in accordance with the relevant guidelines and regulations established by the Research Ethics Committees of the Federal University of Rio Grande do Sul (UFRGS) and the Pontifical Catholic University of Rio Grande do Sul (PUCRS), both located in Porto Alegre, Brazil. The study adhered to Resolution 466/2012 of the National Health Council and the World Medical Association's Code of Ethics, specifically the Declaration of Helsinki. Approval for the project was granted by both UFRGS and PUCRS (CAAE: 38440220.7.3001.5347 and CAAE: 38440220.7.0000.5336, respectively). All participants provided voluntary consent and signed a Free and Informed Consent Form.

Conflicts of Interest

The authors declare no conflicts of interest.

Data Availability Statement

PseudoCell is a free open-source regulatory network available on the PseudoCell website (http://isenesc.com.br/pages/tools.php). Supporting Information tables are available at https://github.com/viniciuspierdona/pseudocell/blob/main/SupplementaryTables.rar.

References

1. V. Gorgoulis, P. D. Adams, A. Alimonti, et al., "Cellular Senescence: Defining a Path Forward," *Cell* 179, no. 4 (2019): 813–827, https://doi.org/10.1016/J.CELL.2019.10.005.

2. A. Hernandez-Segura, J. Nehme, and M. Demaria, "Hallmarks of Cellular Senescence," *Trends in Cell Biology* 28, no. 6 (2018): 436–453, https://doi.org/10.1016/J.TCB.2018.02.001.

3. C. López-Otín, M. A. Blasco, L. Partridge, M. Serrano, and G. Kroemer, "Hallmarks of Aging: An Expanding Universe," *Cell* 186, no. 2 (2023): 243–278, https://doi.org/10.1016/j.cell.2022.11.001.

4. A. Hernandez-Segura, T. V. de Jong, S. Melov, V. Guryev, J. Campisi, and M. Demaria, "Unmasking Transcriptional Heterogeneity in Senescent Cells," *Current Biology: CB* 27, no. 17 (2017): 2652–2660, https://doi.org/10.1016/J.CUB.2017.07.033.

5. M. Bizzarri, A. Palombo, and A. Cucina, "Theoretical Aspects of Systems Biology," *Progress in Biophysics and Molecular Biology* 112, no. 1–2 (2013): 33–43, https://doi.org/10.1016/j.pbiomolbio.2013.03.019.

6. P. V. Coveney and P. W. Fowler, "Modelling Biological Complexity: A Physical Scientist's Perspective," *Journal of the Royal Society Interface* 2, no. 4 (2005): 267–280, https://doi.org/10.1098/RSIF.2005.0045.

7. J. Fisher, N. Piterman, and R. Bodik, "Toward Synthesizing Executable Models in Biology," *Frontiers in Bioengineering and Biotechnology* 2 (2014): 75, https://doi.org/10.3389/FBIOE.2014.00075.

8. T. Helikar, B. Kowal, S. McClenathan, et al., "The Cell Collective: Toward an Open and Collaborative Approach to Systems Biology," *BMC Systems Biology* 6 (2012): 96, https://doi.org/10.1186/1752-0509-6-96.

9. H. Kitano, "Computational Systems Biology," *Nature* 420, no. 6912 (2002): 206–210, https://doi.org/10.1038/nature01254.

10. A. Naldi, "BioLQM: A Java Toolkit for the Manipulation and Conversion of Logical Qualitative Models of Biological Networks," *Frontiers in Physiology* 9 (2018): 1605, https://doi.org/10.3389/FPHYS.2018.01605.

11. M. Ostaszewski, A. Niarakis, A. Mazein, et al., "COVID19 Disease Map, a Computational Knowledge Repository of Virus–Host Interaction Mechanisms," *Molecular Systems Biology* 17, no. 10 (2021): e10387, https://doi.org/10.15252/MSB.202110387.

12. J. Béal, L. Pantolini, V. Noël, E. Barillot, and L. Calzone, "Personalized Logical Models to Investigate Cancer Response to BRAF Treatments in Melanomas and Colorectal Cancers," *PLoS Computational Biology* 17, no. 1 (2021): e1007900, https://doi.org/10.1371/JOURNAL.PCBI.1007900.

13. S. Gupta and R. F. Hashimoto, "Dynamical Analysis of a Boolean Network Model of the Oncogene Role of lncRNA ANRIL and lncRNA

UFC1 in Non-Small Cell Lung Cancer," *Biomolecules* 12, no. 3 (2022): 420, https://doi.org/10.3390/BIOM12030420/S1.

14. S. Gupta, D. A. Silveira, and J. C. M. Mombach, "ATM/miR-34a-5p Axis Regulates a p21-Dependent Senescence-Apoptosis Switch in Non-Small Cell Lung Cancer: A Boolean Model of G1/S Checkpoint Regulation," *FEBS Letters* 594, no. 2 (2020a): 227–239, https://doi.org/10.1002/1873-3468.13615.

15. S. Gupta, D. A. Silveira, and J. C. M. Mombach, "Towards DNA-Damage Induced Autophagy: A Boolean Model of p53-Induced Cell Fate Mechanisms," *DNA Repair* 96 (2020b): 102971, https://doi.org/10.1016/J.DNAREP.2020.102971.

16. O. Rodríguez-Jorge, L. A. Kempis-Calanis, W. Abou-Jaoudé, et al., "Cooperation Between T Cell Receptor and Toll-Like Receptor 5 Signaling for CD4+ T Cell Activation," *Science Signaling* 12, no. 577 (2019): eaar3641, https://doi.org/10.1126/SCISIGNAL.AAR3641.

17. A. Saadatpour and R. Albert, "Boolean Modeling of Biological Regulatory Networks: A Methodology Tutorial," *Methods* 62, no. 1 (2013): 3–12, https://doi.org/10.1016/J.YMETH.2012.10.012.

18. R. Samaga and S. Klamt, "Modeling Approaches for Qualitative and Semi-Quantitative Analysis of Cellular Signaling Networks," *Cell Communication and Signaling* 11, no. 1 (2013): 43, https://doi.org/10.1186/1478-811X-11-43.

19. D. A. Silveira, S. Gupta, and J. C. M. Mombach, "Systems Biology Approach Suggests New miRNAs as Phenotypic Stability Factors in the Epithelial–Mesenchymal Transition," *Journal of the Royal Society Interface* 17, no. 171 (2020): 0693, https://doi.org/10.1098/RSIF.2020.0693.

20. W. Abou-Jaoudé, P. Traynard, P. T. Monteiro, et al., "Logical Modeling and Dynamical Analysis of Cellular Networks," *Frontiers in Genetics* 7 (2016): 1–20, https://doi.org/10.3389/fgene.2016.00094.

21. A. Niarakis and T. Helikar, "A Practical Guide to Mechanistic Systems Modeling in Biology Using a Logic-Based Approach," *Briefings in Bioinformatics* 22, no. 4 (2021): bbaa236, https://doi.org/10.1093/BIB/BBAA236.

22. J. H. Lee and T. T. Paull, "ATM Activation by DNA Double-Strand Breaks Through the Mre11-Rad50-Nbs1 Complex," *Science* 308, no. 5721 (2005): 551–554, https://doi.org/10.1126/science.1108297.

23. E. Riballo, M. Kühne, N. Rief, et al., "A Pathway of Double-Strand Break Rejoining Dependent Upon ATM, Artemis, and Proteins Locating to γ-H2AX Foci," *Molecular Cell* 16, no. 5 (2004): 715–724, https://doi.org/10.1016/j.molcel.2004.10.029.

24. M. A. Serrano, Z. Li, M. Dangeti, et al., "DNA-PK, ATM and ATR Collaboratively Regulate p53-RPA Interaction to Facilitate Homologous Recombination DNA Repair," *Oncogene* 32, no. 19 (2013): 2452–2462, https://doi.org/10.1038/onc.2012.257.

25. B. D. Chang, Y. Xuan, E. V. Broude, et al., "Role of p53 and p21waf1/cip1 in Senescence-Like Terminal Proliferation Arrest Induced in Human Tumor Cells by Chemotherapeutic Drugs," *Oncogene* 18, no. 34 (1999): 4808–4818, https://doi.org/10.1038/SJ.ONC.1203078.

26. J. W. Shay, O. M. Pereira-Smith, and W. E. Wright, "A Role for Both RB and p53 in the Regulation of Human Cellular Senescence," *Experimental Cell Research* 196, no. 1 (1991): 33–39, https://doi.org/10.1016/0014-4827(91)90453-2.

27. Y. A. Hajam, R. Rani, S. Y. Ganie, et al., "Oxidative Stress in Human Pathology and Aging: Molecular Mechanisms and Perspectives," *Cells* 11, no. 3 (2022): 552, https://doi.org/10.3390/CELLS11030552.

28. J. F. Passos, G. Nelson, C. Wang, et al., "Feedback Between p21 and Reactive Oxygen Production Is Necessary for Cell Senescence," *Molecular Systems Biology* 6 (2010): 347, https://doi.org/10.1038/MSB.2010.5.

29. D. P. Gelain, M. A. De Bittencourt Pasquali, C. Comim, et al., "Serum Heat Shock Protein 70 Levels, Oxidant Status, and Mortality in Sepsis," *Shock* 35, no. 5 (2011): 466–470, https://doi.org/10.1097/SHK.0B013E31820FE704.

30. N. Somensi, P. O. Brum, V. De Miranda Ramos, et al., "Extracellular HSP70 Activates ERK1/2, NF-kB and pro-Inflammatory Gene Transcription Through Binding With RAGE in A549 Human Lung Cancer Cells," *Cellular Physiology and Biochemistry: International Journal of Experimental Cellular Physiology, Biochemistry, and Pharmacology* 42, no. 6 (2017): 2507–2522, https://doi.org/10.1159/000480213.

31. D. Furman, J. Chang, L. Lartigue, et al., "Expression of Specific Inflammasome Gene Modules Stratifies Older Individuals Into Two Extreme Clinical and Immunological States," *Nature Medicine* 23, no. 2 (2017): 174–184, https://doi.org/10.1038/NM.4267.

32. I. M. de Toda, N. Ceprián, E. D. Cerro, and M. Del de la Fuente, "The Role of Immune Cells in Oxi-Inflamm-Aging," *Cells* 10, no. 11 (2021): 2974, https://doi.org/10.3390/CELLS10112974.

33. X. Li, C. Li, W. Zhang, Y. Wang, P. Qian, and H. Huang, "Inflammation and Aging: Signaling Pathways and Intervention Therapies," *Signal Transduction and Targeted Therapy* 8, no. 1 (2023): 239, https://doi.org/10.1038/S41392-023-01502-8.

34. N. Basisty, A. Kale, O. H. Jeon, et al., "A Proteomic Atlas of Senescence-Associated Secretomes for Aging Biomarker Development," *PLoS Biology* 18, no. 1 (2020): e3000599, https://doi.org/10.1371/JOURNAL.PBIO.3000599.

35. M. Ohanna, S. Giuliano, C. Bonet, et al., "Senescent Cells Develop a PARP-1 and Nuclear Factor-{Kappa}B-Associated Secretome (PNAS)," *Genes & Development* 25, no. 12 (2011): 1245–1261, https://doi.org/10.1101/GAD.625811.

36. A. L. Barabási and Z. N. Oltvai, "Network Biology: Understanding the Cell's Functional Organization," *Nature Reviews Genetics* 5, no. 2 (2004): 101–113, https://doi.org/10.1038/nrg1272.

37. J. D. Schwab, S. D. Kühlwein, N. Ikonomi, M. Kühl, and H. A. Kestler, "Concepts in Boolean Network Modeling: What Do They all Mean?," *Computational and Structural Biotechnology Journal* 18 (2020): 571, https://doi.org/10.1016/J.CSBJ.2020.03.001.

38. T. Wu, E. Hu, S. Xu, et al., "clusterProfiler 4.0: A Universal Enrichment Tool for Interpreting Omics Data," *Innovations* 2, no. 3 (2021): 100141, https://doi.org/10.1016/j.xinn.2021.100141.

39. G. Yu, L. G. Wang, Y. Han, and Q. Y. He, "ClusterProfiler: An R Package for Comparing Biological Themes Among Gene Clusters," *OMICS: A Journal of Integrative Biology* 16, no. 5 (2012): 284–287, https://doi.org/10.1089/OMI.2011.0118.

40. M. E. Ritchie, B. Phipson, D. Wu, et al., "Limma Powers Differential Expression Analyses for RNA-Sequencing and Microarray Studies," *Nucleic Acids Research* 43, no. 7 (2015): e47, https://doi.org/10.1093/NAR/GKV007.

41. P. Dumont, M. Burton, Q. M. Chen, et al., "Induction of Replicative Senescence Biomarkers by Sublethal Oxidative Stresses in Normal Human Fibroblast," *Free Radical Biology & Medicine* 28, no. 3 (2000): 361–373, https://doi.org/10.1016/S0891-5849(99)00249-X.

42. E. R. Westin, N. Aykin-Burns, E. M. Buckingham, D. R. Spitz, F. D. Goldman, and A. J. Klingelhutz, "The p53/p21WAF/CIP Pathway Mediates Oxidative Stress and Senescence in Dyskeratosis Congenita Cells With Telomerase Insufficiency," *Antioxidants & Redox Signaling* 14, no. 6 (2011): 985, https://doi.org/10.1089/ARS.2010.3444.

43. W. S. El-Deiry, T. Tokino, V. E. Velculescu, et al., "WAF1, a Potential Mediator of p53 Tumor Suppression," *Cell* 75, no. 4 (1993): 817–825, https://doi.org/10.1016/0092-8674(93)90500-P.

44. J. Loughery, M. Cox, L. M. Smith, and D. W. Meek, "Critical Role for p53-Serine 15 Phosphorylation in Stimulating Transactivation at p53-Responsive Promoters," *Nucleic Acids Research* 42, no. 12 (2014): 7666–7680, https://doi.org/10.1093/NAR/GKU501.

45. M. C. Marazita, A. Dugour, M. D. Marquioni-Ramella, J. M. Figueroa, and A. M. Suburo, "Oxidative Stress-Induced Premature Senescence Dysregulates VEGF and CFH Expression in Retinal Pigment

Epithelial Cells: Implications for Age-Related Macular Degeneration," *Redox Biology* 7 (2016): 78–87, https://doi.org/10.1016/J.REDOX.2015.11.011.

46. C. Mas-Bargues, J. Viña-Almunia, M. Inglés, et al., "Role of p16INK4a and BMI-1 in Oxidative Stress-Induced Premature Senescence in Human Dental Pulp Stem Cells," *Redox Biology* 12 (2017): 690–698, https://doi.org/10.1016/J.REDOX.2017.04.002.

47. A. Salminen, A. Kauppinen, and K. Kaarniranta, "Emerging Role of NF-κB Signaling in the Induction of Senescence-Associated Secretory Phenotype (SASP)," *Cellular Signalling* 24, no. 4 (2012): 835–845, https://doi.org/10.1016/J.CELLSIG.2011.12.006.

48. M. Serrano, A. W. Lin, M. E. McCurrach, D. Beach, and S. W. Lowe, "Oncogenic Ras Provokes Premature Cell Senescence Associated With Accumulation of p53 and p16(INK4a)," *Cell* 88, no. 5 (1997): 593–602, https://doi.org/10.1016/S0092-8674(00)81902-9.

49. A. Alimonti, C. Nardella, Z. Chen, et al., "A Novel Type of Cellular Senescence That Can Be Enhanced in Mouse Models and Human Tumor Xenografts to Suppress Prostate Tumorigenesis," *Journal of Clinical Investigation* 120, no. 3 (2010): 681–693, https://doi.org/10.1172/JCI40535.

50. M. V. Astle, K. M. Hannan, P. Y. Ng, et al., "AKT Induces Senescence in Human Cells via mTORC1 and p53 in the Absence of DNA Damage: Implications for Targeting mTOR During Malignancy," *Oncogene* 31, no. 15 (2012): 1949–1962, https://doi.org/10.1038/ONC.2011.394.

51. K. T. Chan, S. Blake, H. Zhu, et al., "A Functional Genetic Screen Defines the AKT-Induced Senescence Signaling Network," *Cell Death and Differentiation* 27, no. 2 (2019): 725–741, https://doi.org/10.1038/s41418-019-0384-8.

52. A. Di Leonardo, S. P. Linke, K. Clarkin, and G. M. Wahl, "DNA Damage Triggers a Prolonged p53-Dependent G1 Arrest and Long-Term Induction of Cip1 in Normal Human Fibroblasts," *Genes & Development* 8, no. 21 (1994): 2540–2551, https://doi.org/10.1101/GAD.8.21.2540.

53. F. M. Barbé-Tuana, L. K. Grun, V. Pierdoná, et al., "Shorter Telomeres in Children With Severe Asthma, an Indicative of Accelerated Aging," *Aging* 13, no. 2 (2021): 1686–1691, https://doi.org/10.18632/AGING.202527.

54. J. Hoefer, M. Luger, C. Dal-Pont, Z. Culig, H. Schennach, and S. Jochberger, "The "Aging Factor" Eotaxin-1 (CCL11) is Detectable in Transfusion Blood Products and Increases With the Donor's Age," *Frontiers in Aging Neuroscience* 9 (2017): 402, https://doi.org/10.3389/FNAGI.2017.00402.

55. A. P. Badewa and A. S. Heiman, "Inhibition of CCL11, CCL24, and CCL26-Induced Degranulation in HL-60 Eosinophilic Cells by Specific Inhibitors of MEK1/MEK2, p38 MAP Kinase, and PI 3-Kinase," *Immunopharmacology and Immunotoxicology* 25, no. 2 (2003): 145–157, https://doi.org/10.1081/IPH-120020466.

56. G. T. Kampen, S. Stafford, T. Adachi, et al., "Eotaxin Induces Degranulation and Chemotaxis of Eosinophils Through the Activation of ERK2 and p38 Mitogen-Activated Protein Kinases," *Blood* 95, no. 6 (2000): 1911–1917, https://doi.org/10.1182/BLOOD.V95.6.1911.

57. T. Miyagaki, M. Sugaya, T. Murakami, et al., "CCL11-CCR3 Interactions Promote Survival of Anaplastic Large Cell Lymphoma Cells via ERK1/2 Activation," *Cancer Research* 71, no. 6 (2011): 2056–2065, https://doi.org/10.1158/0008-5472.CAN-10-3764.

58. J. Y. Park, Y. W. Kang, B. Y. Choi, Y. C. Yang, B. P. Cho, and W. G. Cho, "CCL11 Promotes Angiogenic Activity by Activating the PI3K/Akt Pathway in HUVECs," *Journal of Receptor and Signal Transduction Research* 37, no. 4 (2017): 416–421, https://doi.org/10.1080/10799893.2017.1298132.

Supporting Information

Additional supporting information can be found online in the Supporting Information section.